SPANDIDOS PUBLICATIONS

MOLECULAR MEDICINE REPORTS 18: 4657-4665, 2018

Sevoflurane-induced neurotoxicity is driven by OXR1 post-transcriptional downregulation involving hsa-miR-302e

LEILEI YANG, QIAN SHEN, YANQIONG XIA, XUEHENG LEI and JIAN PENG

Department of Anesthesiology, Tongren Hospital of Wuhan University (Wuhan Third Hospital), Wuhan, Hubei 430060, P.R. China

Received November 4, 2017; Accepted April 13, 2018

DOI: 10.3892/mmr.2018.9442

Abstract. Sevoflurane is a common anesthetic agent used in surgical settings and previous studies have indicated that it exerts a neurotoxic effect. However, the molecular mechanism underlying this side effect is unknown. In addition, the human microRNA-302 (hsa-miR-302) family members have been reported to be involved in neuronal cell development and biology. Thus, the present study aimed to investigate the potential implication of hsa-miR-302e in the sevoflurane-induced cytotoxicity on human hippocampal cells (HN-h). HN-h cells were transfected with hsa-miR-302e mimic, hsa-miR-302e inhibitor or negative controls and subsequently exposed to different concentrations of sevoflurane. An MTT assay was used to assess the cytotoxicity of sevoflurane on HN-h cells. Cell apoptosis was determined by flow cytometry. The levels of lactate dehydrogenase release, reactive oxygen species, lipid peroxidation and intracellular calcium (Ca^{2+}) were additionally detected. Reverse transcription-quantitative polymerase chain reaction and western blotting were conducted to determine mRNA and protein expression, respectively. A luciferase assay was performed for validating the targeting of OXR1 by hsa-miR-302e. The results indicated that sevoflurane induced a decrease in cell viability, malondialdehyde and reactive oxygen species production, lactate dehydrogenase release, intracellular Ca^{2+} production, calcium/calmodulin-dependent protein kinase II phosphorylation and apoptosis. In addition, treatment with sevoflurane induced the expression of hsa-miR-302e while the expression of its target, oxidation resistance gene 1 (OXR1), was significantly downregulated. Inhibition of hsa-miR-302e expression protected neuronal cells from sevoflurane cytotoxicity. Mechanistic studies demonstrated that OXR1 was a direct target of hsa-miR-302e. Furthermore, the overexpression of OXR1 abolished the effect of sevoflurane on neuronal cells. The results of the present study indicated that sevoflurane exerts its neurotoxic effect by regulating the hsa-miR-302e/OXR1 axis. Therefore, the manipulation of the hsa-miR-302e/OXR1 pathway will be useful for preventing sevoflurane-induced neurotoxicity.

Correspondence to: Dr Jian Peng, Department of Anesthesiology, Tongren Hospital of Wuhan University (Wuhan Third Hospital), 216 Guanshan Avenue, Wuhan, Hubei 430060, P.R. China
E-mail: 137585260@qq.com

Key words: sevoflurane, neurotoxicity, neuronal cells, hsa-microRNA-302e, oxidation resistance gene 1

Introduction

Sevoflurane is a volatile anesthetic used to induce and maintain general anesthesia in surgical settings. It is one of the most commonly used anesthetic agents that progressively eclipsed a number of existing anesthetics since its first use as an anesthetic agent. It owes its popularity to its low airway irritability, ability to rapidly induce anesthesia and good pharmacokinetic performance (1-3). However, growing evidence demonstrates that sevoflurane caused severe side effects, particularly in infants (4,5). Indeed, sevoflurane was reported to induce high rates of postoperative cognitive dysfunction in comparison with other anesthetic agents (6). These dysfunctions may be associated with sevoflurane-induced neurotoxicity, which is documented in animals and humans (7-9). To date, the molecular mechanisms underlying sevoflurane-induced neurotoxicity have not been fully elucidated. However, a number of studies have demonstrated that exposure to sevoflurane induces alterations in the microRNA (miR) expression profile (10-14).

miRs are small non-coding RNA molecules involved in the regulation of a number of biological processes. They principally act as post-transcriptional gene regulators by binding to complementary sequences of target mRNAs, which leads to mRNA silencing via the inhibition of translation or destabilization of the mRNAs (15,16). miRs are expressed in response to particular conditions including exposure to anesthetic agents such as sevoflurane (12,17). Thousands of miR species have been identified, sequenced and characterized; however, their functional roles have yet to be clarified, as one miR may regulate the expression of a number of genes, including other gene regulators. The human miR-302 family members have been demonstrated to be involved in neuronal cell development and biology (18,19). The miR-302/367 cluster, including miR-367, miR-302a, miR-302b, miR-302c and miR-302d, has been reported to serve crucial roles in a variety of biological processes, including the pluripotency of human embryonic stem cells (20), reprogramming and self-renewal (21), tumor growth (22) and the regulation of

hypoxia (23). It was additionally demonstrated that miR-302 is involved in the regulation of neurulation by inhibiting the differentiation and expansion of neural progenitors (24). miR-302 is known to regulate DNA repair within cells (25). In addition, the miR-302/367 cluster is able to orchestrate processes involved in neural tube formation (26). Notably, a previous study have indicated that miR-302 protects cells from cytotoxicity by activating the protein kinase B/nuclear factor erythroid 2-related factor 2/Nanog axis, to subsequently improve insulin signaling in neurons (27). An additional study has demonstrated that miR-302 antagomir protects cells from apoptosis in hypoxia/reoxygenation injury (28). Additionally, miR-302/367 has crucial roles in the regeneration of the hippocampus and other brain structures following neuronal loss (29) and may restore learning and memory in patients with Alzheimer's disease (30). Therefore, miR-302 family members were hypothesized to be involved in sevoflurane-induced neurotoxicity.

Among the miR-302 family members, miR-302e is the least studied and its functional role is unknown. The present study aimed to experimentally document the *in vitro* neurotoxic effect of sevoflurane and the role of hsa-miR-302e in the underlying mechanism.

Materials and methods

Cell culture. Human neurons-hippocampal primary cells (HN-h; cat. no. 1540) were purchased from ScienCell Research Laboratories, Inc. (San Diego, CA, USA) and plated in Neuronal Medium (cat. no. 1521), additionally from ScienCell Research Laboratories, Inc. As recommended by the manufacturer, cells were cultured at 37˚C in an environment of 95% humidity and 5% CO_2 incubator for 48 h.

Transient transfection. HN-h cells ($5x10^4$ cells/cm^2) were transfected with 5 nM hsa-miR-302e mimic (5'-UAAGUG CUUCCAUGCUU-3'; MISSION® microRNA mimic), 20 nM hsa-miR-302e inhibitor (5'-UAAGUGCUUCCAUGCUU-3') or respective controls (control mimic oligonucleotide, 5'-UCA CAACCUCCUAGAAAGAGUAGA-3'; control inhibitor oligonucleotide, 5'-UUGUACUACACAAAAGUACUG-3'; Thermo Fisher Scientific, Inc., Waltham, MA, USA) using Lipofectamine® reagent (Thermo Fisher Scientific, Inc.) according to the manufacturer's protocol. For oxidation resistance gene 1 (OXR1) overexpression, the OXR1 Lentiviral vector (Human; CMV; pLenti-GIII-CMV) was purchased from Applied Biological Materials Inc. (Richmond, BC, Canada) and was employed for transfection following the manufacturer's protocol. A reverse transcription-quantitative polymerase chain reaction (RT-qPCR) was used to verify the transfection efficiency 72 h following transfection.

Exposure to sevoflurane. Sevoflurane exposure experiments was performed as previously described with minor modifications (31). Briefly, hermetically sealed plastic chambers were used. The chamber was equipped with an inlet connector coupled to a sevoflurane vaporizer and an outlet connector linked to a gas monitor (PM 8060; Drager AG & Co., KGaA, Lübeck, Germany), which was necessary for checking the gas concentration in the chamber. Cell cultures (10^5 cells/well) were kept in the chambers and following the adjustment of sevoflurane concentration, each chamber was treated with 0, 5, 10 or 15% sevoflurane in the carrier gas (95% air/5% CO_2) for 15 min. Subsequently, once a target concentration was attained, the corresponding chamber was sealed and incubated for 6 h at 37˚C with renewal of the gas in the chamber every 3 h. The gas monitor was used to confirm the target concentration of sevoflurane at the end of the experiment. For control cells, the same procedure was applied with substitution of sevoflurane by 5% CO_2 air.

Cell viability. An MTT assay was used to evaluate the cytotoxic effect of sevoflurane on the viability of HN-h cells. Following the 6 h sevoflurane exposure, cells were subsequently cultured for a period of 48 h prior to the addition of 20 μl MTT reagent (Cell Proliferation kit I; Roche Applied Science, Penzberg, Germany; 5 mg/ml). Subsequently, the mixture was incubated for an additional 4 h prior to the removal of culture supernatants and their replacement in each well with 150 μl DMSO as a solubilizing reagent for the formazan crystals produced by viable cells. Finally, cell viability was spectrophotometrically assessed via measuring the optical density at 570 nm with a spectrophotometer (Spectronic Genesys-5; Milton Roy; Accudyne Industries, Dallas, TX, USA).

Apoptosis assay. A FITC-Annexin V/7-AAD kit (Beckman Coulter, Inc., Brea, CA, USA) was used for apoptosis analysis. Following incubation, ~$1x10^5$ cells were collected and rinsed twice using PBS prior to Annexin V/7-AAD staining for 15 min at room temperature. Subsequently, cell apoptosis was analyzed using a flow cytometer (BD Biosciences, Franklin Lakes, NJ, USA; C6). The software used for analyzing the data was BD FACSDiva software v8.0.1 (BD Biosciences). Three independent experiments were performed.

Determination of lactate dehydrogenase (LDH) release. The culture medium (10^5 cells/cm^2) was taken from the wells and spun in a microfuge for 2 min at 4˚C and 15,000 x g to remove any detached debris. The supernatant was collected for the measurement of LDH in the cell-free medium. The cell pellet and the cells remaining in the multiwell were lysed in 0.5 ml lysis buffer [0.5% Triton X-100 in 0.1 M potassium phosphate buffer, (pH 7.0)]. LDH activity was assessed using a colorimetric method by monitoring the absorbance at 340 nm in the presence of 0.2 mM NADH and 2 mM pyruvate. A total of 1 unit of LDH activity is defined as the amount of enzyme that catalyzes the formation of 1 μmol NAD mm^{-1} under the assay conditions and the percentage of LDH released was estimated as the cell-free LDH activity divided by the total LDH activity.

Reactive oxygen species (ROS) level detection. To determine the level of ROS produced by the cells, cells were collected, rinsed three times with PBS and trypsinized prior to centrifugation at 4˚C and 15,000 x g for 10 min. Collected cells were incubated with diluted dihydroethidium provided with the Reactive Oxygen Detection kit (cat. no. S0033) purchased from Beyotime Institute of Biotechnology (Haimen, China) according to the manufacturer's protocol. Subsequently, the level of ROS was evaluated by flow cytometry analysis using the software mentioned above.

Lipid peroxidation assay. To determine the extent of lipid peroxidation, cells were harvested via centrifugation at 4˚C and 15,000 x g for 15 min. The collected cells were frozen and subsequently thawed. Following thawing, 1 ml 0.67% thiobarbituric acid (TBA; Wako Pure Chemical Industries, Ltd., Osaka, Japan) and 0.4 ml 5% trichloroacetic acid were added to the cell suspensions, followed by heating of the mixture for 60 min in a boiling water bath. Then, the mixture was centrifuged at 4˚C and 15,000 x g for 15 min and the absorbance measured at 532 nm with a spectrophotometer (Spectronic Genesys-5; Milton Roy; Accudyne Industries). The amount of malondialdehyde (MDA) was deduced from the molar extinction coefficient of the MDA-TBA complex of $1.56x10^5$ cm^{-1} M^{-1}.

Measurement of intracellular Ca^{2+}. In order to measure the intracellular Ca^{2+}, the Fluo 3-AM reagent (Thermo Fisher Scientific, Inc.) was used. Cells were cultured with 5 mM glutamate in the presence or absence of sevoflurane. Following harvesting, cells were incubated at 37˚C for 30 min with Fluo 3-AM. Subsequently, Ca^{2+}-dependent fluorescence intensity was measured by flow cytometry and 10,000 cells were acquired and analyzed for each sample.

RT-qPCR analysis. RNA was isolated using miRNA Isolation kit or miRNeasy Mini kit (Qiagen GmbH, Hilden, Germany) following the manufacturer's protocol, and cDNA synthesis was performed with the TaqMan MicroRNA Reverse Transcription kit (Thermo Fisher Scientific, Inc.). Subsequently, the qPCR amplification was achieved using the hsa-miR-302e primers with the CFX96 Touch™ Real-Time PCR Detection System (Bio-Rad Laboratories, Inc., Hercules, CA, USA) according to the manufacturer's protocol. The forward and reverse primers sequences for the hsa-miR-302e were; forward primer, 5'-CGC AGTAAGTGCTTCCA-3' and reverse primer, 5'-GTCCAG TTTTTTTTTTTTTTTAAGCAT-3'. The primers for U6 gene were; forward primer, 5'-GTGCTCGCTTCGGCAGCA CATATAC-3' and reverse primer, 5'-AAAAATATGGAA CGCTTCACGAATTTG-3'. The primers for OXR1 were forward primer, 5'-TTCGACCAAACCTAAGTGATCCC-3' and reverse primer, 5'-GGGGTGTCTAAACCTGTCATT G-3'. The primers for GAPDH were forward primer, 5'-ACC CACTCCTCCACCTTTGA-3' and reverse primer, 5'-CTG TTGCTGTAGCCAAATTCGT-3' The PCR conditions were: 30 sec at 95˚C, 45 amplification cycles at 95˚C for 5 sec and 58˚C for 34 sec. The expression level hsa-miR-302e was obtained using the $2^{-\Delta\Delta Cq}$ method (32) with U6 small nuclear RNA as a normalizing control while GAPDH was used as internal control for OXR1.

Western blot analysis. HN-h cells were collected with trypsin and lysed with radioimmunoprecipitation assay buffer (Sigma-Aldrich; Merck KGaA, Darmstadt, Germany) and protein concentration in cell lysates were measured using the bicinchoninic acid protein assay kit (Beyotime Institute of Biotechnology). Next, 50 μg of the lysates were purified by 10% SDS-PAGE and subsequently transferred to polyvinylidene difluoride membranes. Following blocking at 4˚C with 5% bovine serum albumin in Tris-buffered saline with 0.05% Tween-20 (TBST) for 2 h, the membranes were incubated at 4˚C overnight with primary antibodies against OXR1 (cat. no. HPA027375; dilution 1:1,000; Sigma-Aldrich; Merck KGaA), Phospho-CaMKII (Thr286; cat. no. D21E4; dilution 1:1,000; Cell Signaling Technology, Inc., Danvers, MA, USA), CaMKII-α (cat. no. D10C11; dilution 1:1,000; Cell Signaling Technology, Inc.) and GAPDH (cat. no. ab9485; dilution 1:1,000; Abcam, Cambridge, UK) overnight at 4˚C. Next, the membranes were washed three times with TBST for 5 min and incubated with horseradish peroxidase conjugated anti-mouse mouse anti-human immunoglobulin M antibody (M11; cat. no. sc-66121; 1:1,000; Santa Cruz Biotechnology, Inc., Dallas, TX, USA) at room temperature for 1 h, followed by 5 min wash with TBST, which was repeated three times. The membranes were visualized using The Clarity Western Enhanced Chemiluminescent Substrate (cat. no. 1705060; Bio-Rad Laboratories, Inc.). Densitometric analysis was achieved using the Image J software version 1.51k (National Institutes of Health, Bethesda, MD, USA) for Windows.

Bioinformatics. The online bioinformatics tool Targetscan (http://www.targetscan.org) was used for predicting the targeting of OXR1 by hsa-miR-302e.

Luciferase assays. The 3'-untranslate region (UTR) of OXR1 was isolated and 50 μg was used for cloning into the *Renilla* luciferase plasmid pRL-TK vector (Promega Corporation, Madison, WI, USA) in the downstream region of the *Renilla* luciferase gene. Additionally, the mutated 3'-UTR of OXR1 (pRL-TK /OXR1-Mut) was produced with the QuikChange II Site-Directed Mutagenesis kit purchased from Agilent Technologies, Inc. (Santa Clara, CA, USA). For the luciferase assays, HN-h cells were seeded in 24-well plates at a density of 10^5 cells/well and co-transfected with miR-302e mimic (5 nM) and 10 ng of pRL-TK vector (Promega Corporation) and the *Renilla* luciferase plasmid pRL-TK vector (10 ng) [luciferase gene under the control of OXR1 UTR] using Lipofectamine® 2000 (Invitrogen; Thermo Fisher Scientific, Inc.). Cells were collected 48 h following transfection and lysed prior to the measurement of luciferase activity with the Dual-Luciferase Reporter Assay System (Promega Corporation). *Renilla* luciferase was used for normalization. The experiments were performed independently in triplicate.

Statistical analysis. GraphPad Prism software (version 6.0; GraphPad Software, Inc., La Jolla, CA, USA) was used for statistical analysis. Each data was presented as the mean ± standard deviation. Statistical differences were evaluated using one-way or two-way analysis of variance followed by Dunnett's multiple comparisons test. All experiments were performed at least three times. $P<0.05$ was considered to indicate a statistically significant difference.

Results

Sevoflurane exerts a cytotoxic effect on HN-h cells. HN-h cells were incubated for 6 h in the presence of sevoflurane at different concentrations and cell viability was monitored by MTT assay after 48 h of incubation in culture medium. The cell viability was decreased in a dose-dependent manner in presence of sevoflurane. At 5% sevoflurane, cell viability was

significantly decreased to 88.35±2.1% (P<0.01) compared with the control. In presence of 15% sevoflurane, cell viability was significantly reduced to 39.85±4% (P<0.0001) compared with the control cells (Fig. 1A; Table I). To further understand the mechanism of this decrease in cell viability, the level of apoptosis was also determined following incubation of cells in the presence (15% sevoflurane) or absence of sevoflurane. In the absence of sevoflurane, the apoptosis rate was estimated to be 0.11±0.08 (n=3). The apoptosis rate significantly increased to 9.25±1.5 in cell cultures incubated with 15% sevoflurane (Fig. 1B; P<0.0001 vs. 0%). Markers of apoptotic pathways were additionally investigated in the cells cultured in the absence or presence of various concentrations of sevoflurane (Fig. 1C-G). The results indicated that sevoflurane significantly increased LDH and intracellular Ca^{2+} release in a dose-dependent manner (P<0.01; Fig. 1C and F). The level of ROS and MDA were also increased by sevoflurane (Fig. 1D and E). The level of calcium/calmodulin-dependent protein kinase II (CAMII) did not significantly alter but the level of phosphorylated CAMII was significantly increased by sevoflurane exposure (P<0.01; Fig. 1G).

Sevoflurane upregulates hsa-miR-302e in HN-h cells. RT-qPCR experiments were performed to determine the level of hsa-miR-302e in cultured cells. The results revealed a dose-dependent increase in hsa-miR-302e expression following treatment with sevoflurane (Fig. 2A). The levels of hsa-miR-302e were significantly increased to 2.42±0.60 (P<0.01), 3.98±0.40 (P<0.001) and 8.40±0.32 (P<0.0001) in the 5, 10 and 15% groups, respectively compared with the control group (1.03±0.20). These results suggested a potential role of hsa-miR-302e in sevoflurane-induced cytotoxicity.

Inhibition of hsa-miR-302e alleviates sevoflurane-induced cytotoxicity. In order to study the involvement of hsa-miR-302e in sevoflurane-induced cytotoxicity, cells were transfected with the hsa-miR-302e mimic or its inhibitor, which efficiently upregulated or downregulated the expression of hsa-miR-302e in cells, respectively (Fig. 2B). The cells were subsequently subjected to 15% sevoflurane and the results are presented in Fig. 2C-I. The overexpression of hsa-miR-302e significantly reduced cell viability from 100 to 58.12±2.10% (P<0.0001; Fig. 2C) and significantly induced cell apoptosis (Fig. 2D; P<0.0001). Additionally, the hsa-miR-302e mimic significantly induced ROS production (Fig. 2E; P<0.01), LDH release (Fig. 2F; P<0.01), increased MDA content (Fig. 2G; P<0.0001), intracellular Ca^{2+} level (Fig. 2H; P<0.0001) and CAMII phosphorylation (Fig. 2I; P<0.0001). In addition, hsa-miR-302e inhibitor induced the opposite trends and even increased cell viability in comparison with the controls.

OXR1 is a direct target of hsa-miR-302e. The online Targetscan tool predicted that OXR1 was among the candidate targets of hsa-miR-302e (Fig. 3A). Given that oxidative stress pathways were activated by sevoflurane, western blot analysis was performed to investigate the effect of sevoflurane on OXR1 expression. The results demonstrated that treatment with sevoflurane significantly reduced the level of OXR1 protein in a dose-dependent manner (Fig. 3B; P<0.01).

Table I. Sevoflurane-induced cytotoxic effect.

Concentration of sevoflurane, %	Cell viability, %	Apoptosis rate, %	LDH leakage, %	$[Ca^{2+}]i$, μM	ROS production, %	MDA, mmol/200 μl	CAMII expression level[a]	p-CAMII expression level[a]
0	100.000±1.000	0.190±0.080	12.300±1.500	0.018±0.002	8.650±0.500	4.230±0.910	0.360±0.050	0.250±0.030
5	88.350±2.100		33.480±2.100	0.222±0.030		4.790±0.500	0.360±0.020	0.600±0.031
10	65.140±3.500		55.300±2.850	0.598±0.010		6.490±0.300	0.380±0.010	0.770±0.040
15	39.850±4.000	25.900±1.500	71.200±3.200	0.926±0.025	12.100±1.000	10.610±0.600	0.390±0.030	0.970±0.020

[a]Protein expression relative to GAPDH. LDH, lactate dehydrogenase; i, intracellular; ROS, reactive oxidative species; MDA, malondialdehyde; CAMII, calcium/calmodulin-dependent protein kinase II; p, phospho.

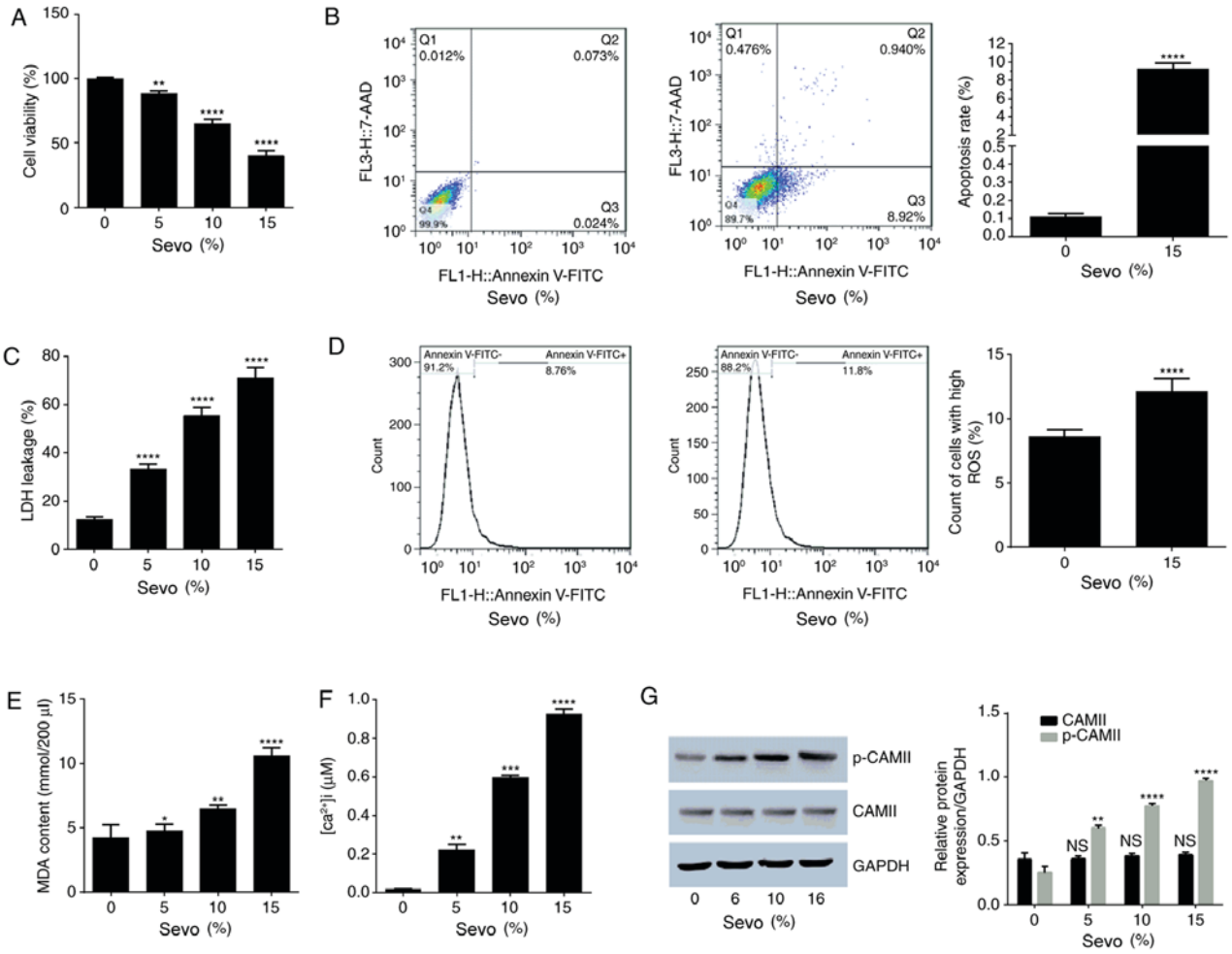

Figure 1. Sevo exerted cytotoxic effects on HN-h cells. The effect of 6 h treatment with varying concentrations of sevo was measured. (A) Cell viability determined using an MTT assay. (B) Apoptosis rate with flow cytometry results. (C) Level of LDH leakage. (D) ROS count. (E) Results of lipid peroxidation assay (MDA content). (F) Concentration of intracellular Ca^{2+}. (G) Western blotting evaluation of the expression level of CAMII and phosphorylated CAMII relative to GAPDH. *P<0.05, **P<0.01, ***P<0.001, ****P<0.0001 vs. control (0% Sevo group). Sevo, sevoflurane; LDH, lactate dehydrogenase; FITC, fluorescein isothiocyanate; ROS, reactive oxygen species; $[Ca^{2+}]$i, intracellular calcium; MDA, malondialdehyde; p-, phospho-; CAMII, calcium/calmodulin-dependent protein kinase II; NS, no significance.

The expression level of the luciferase reporter gene fused to OXR1 3'-UTR in control cells and cells harboring the hsa-miR-302e mimic or inhibitor was presented in Fig. 3C. The hsa-miR-302e mimic significantly reduced the expression level of the reporter gene (P<0.0001) whereas the hsa-miR-302e inhibitor led to significantly upregulated OXR1 expression (P<0.0001). No significant difference was demonstrated with the mutated 3'-UTR vector (Fig. 3C). Furthermore, western blot analysis indicated that hsa-miR-302e overexpression significantly downregulated OXR1 expression (Fig. 3D; P<0.0001). These results demonstrated that OXR1 is a direct target of hsa-miR-302e. The expression of OXR1 was significantly increased following transfection with the overexpression vector, which suggested a good transfection efficiency (Fig. 3E; P<0.0001).

Overexpression of OXR1 abolishes sevoflurane-induced cytotoxicity. OXR1-overexpressing cells were used to study the role of OXR1 in sevoflurane-induced cytotoxicity. The OXR1-overexpressing cells were treated with 15% sevoflurane and the results of its effects are presented in Fig. 4. OXR1-overexpressing cells demonstrated a significant increase in viability following sevoflurane exposure compared with the control cells (P<0.0001; Fig. 4A). In addition, a reduced apoptotic rate and reduced levels of cytotoxicity markers were observed in cells overexpressing OXR1 (Fig. 4B-G). These results suggested that overexpression of OXR1 abrogated sevoflurane-induced cytotoxicity.

Discussion

Sevoflurane has gained interest due to a number of advantages over other anesthetics, however its use also has certain limitations, including neuronal cytotoxicity. This cytotoxicity has been documented in several studies (7,33). HN-h cells were used in the present study as an *in vitro* model to analyze the cytotoxic effect of sevoflurane on the human brain. The results confirmed that sevoflurane is toxic to hippocampal neuronal cells following 6 h of exposure and pointed to oxidative stress as the principal trigger in sevoflurane-induced neurotoxicity. The detection of MDA and the release of LDH demonstrated that the oxidative stress induced by sevoflurane leads to

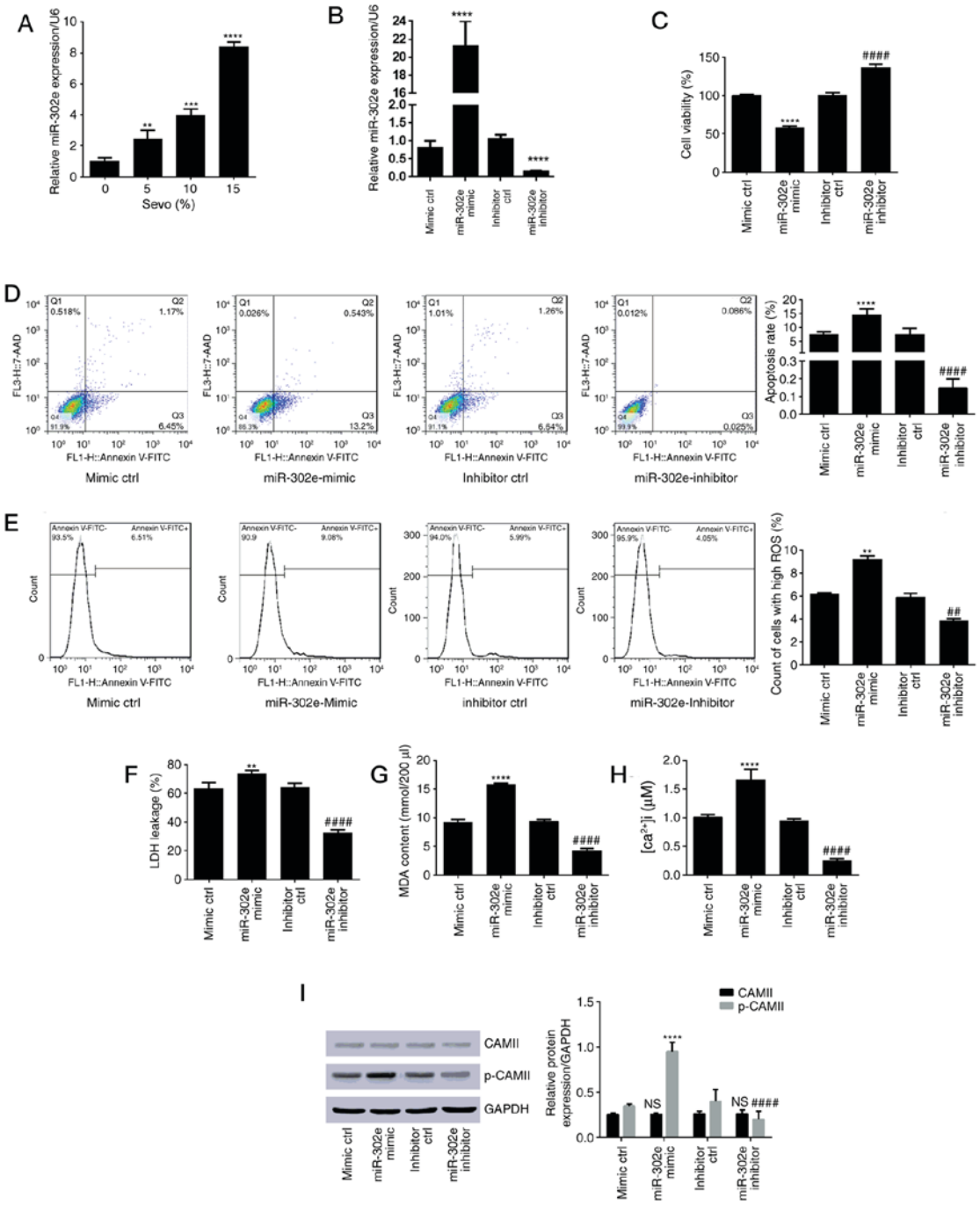

Figure 2. Sevo upregulated hsa-miR-302e in HN-h cells and inhibition of hsa-miR-302e alleviated sevo-induced cytotoxicity. (A) Expression level of hsa-miR-302e following cell treatment with sevo was measured using the reverse transcription-quantitative polymerase chain reaction approach. **P<0.01, ***P<0.001, ****P<0.0001 vs. control (0% Sevo group). (B) Expression level of hsa-miR-302e following transfection with mir-302e mimic, inhibitor or corresponding negative controls was measured using the reverse transcription-quantitative polymerase chain reaction approach. (C) Cell viability determined using MTT assay. (D) Apoptosis rate with flow cytometry results. (E) ROS count. (F) Level of LDH leakage. (G) Results of lipid peroxidation assay (MDA content). (H) Concentration of intracellular Ca^{2+}. (I) Expression level of CAMII and p-CAMII relative to GAPDH. **P<0.01, ***P<0.001, ****P<0.0001 vs. mimic control; $^{##}$P<0.01, $^{####}$P<0.0001 vs. the inhibitor control. Sevo, sevoflurane; miR, microRNA; ctrl, control; 7-AAD, 7-aminoactinomycin D; FITC, fluorescein isothiocyanate; ROS, reactive oxygen species; LDH, lactate dehydrogenase; MDA, malondialdehyde; $[Ca^{2+}]i$, intracellular calcium; CAMII, calcium/calmodulin-dependent protein kinase II; p-, phospho-; NS, no significance.

membrane disruption and necrosis. In addition, apoptotic molecular markers were also detected demonstrating that the cytotoxic effect of sevoflurane occurs by activating apoptosis signaling pathways.

Oxidative stress is one of the most common events associated with cytotoxic effects in the central nervous system. It is observed in sclerosis, Alzheimer's and Parkinson's disease (34). This demonstrates the necessity to maintain an oxidative equilibrium in neuronal cells. OXR1 occupies a crucial role among the various molecules that prevent neuronal cells from oxidation stress-associated death (35). This eukaryotic, highly conserved protein does not scavenge ROS, it regulates the molecular pathways that allow cell protection against oxidative stress and neurodegenerative

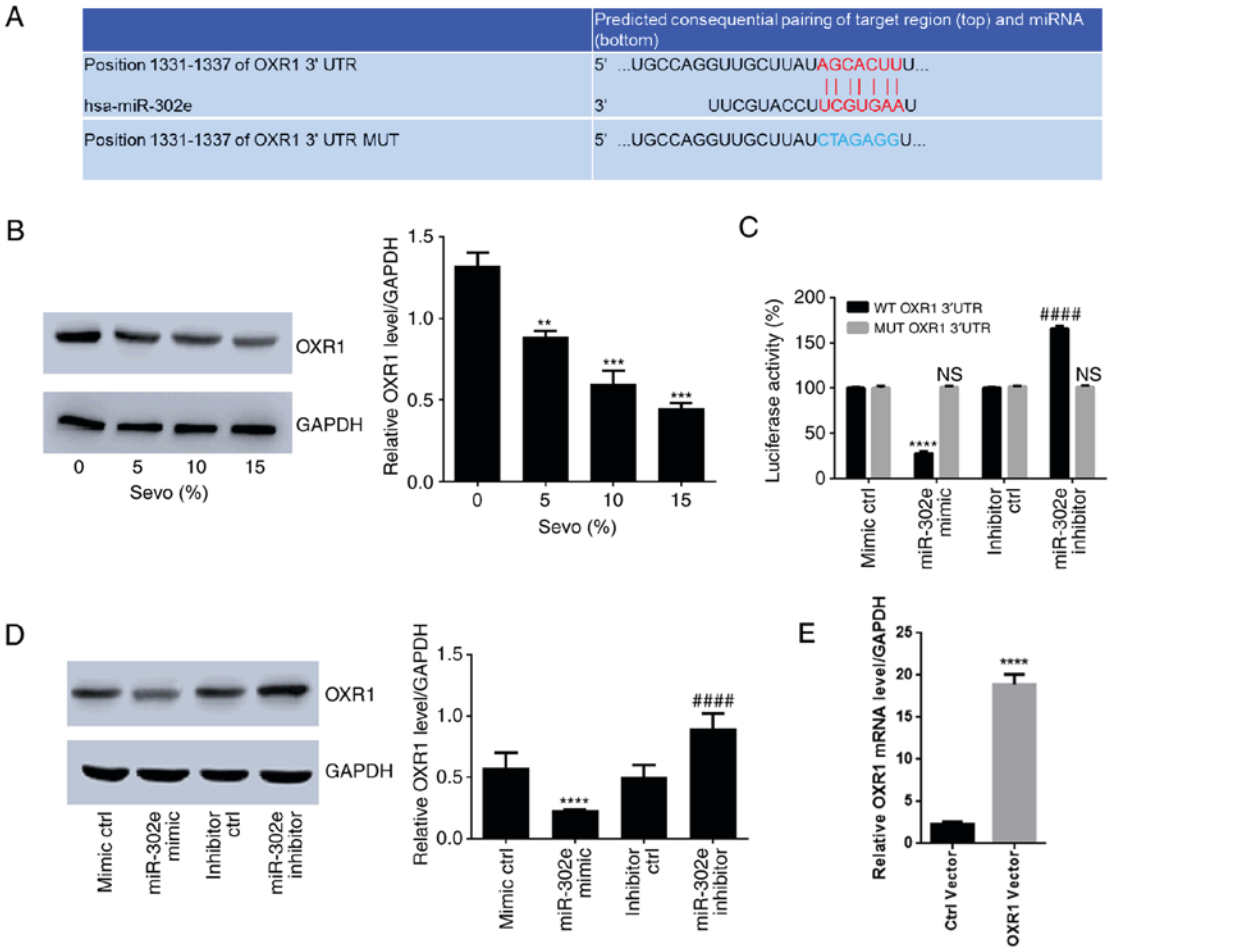

Figure 3. OXR1 is a specific target of hsa-miR-302e. (A) Alignment of the hsa-miR-302e sequence with its target sequence in OXR1 UTR region as predicted by Targetscan. **P<0.01, ***P<0.001 vs. the control (0% Sevo). (B) Expression level of OXR1 following treatment with sevo. (C) Results of luciferase reporter gene assay. (D) Expression level of OXR1 in cells transfected with hsa-miR-302e mimic or inhibitor. (E) Expression level of OXR1 in cells transfected with OXR1 expression vector. *P<0.05, **P<0.01, ***P<0.001, ****P<0.0001 vs. the mimic control; $^{####}$P<0.0001 vs. the inhibitor control. OXR1, oxidation resistance gene 1; UTR, untranslated region; miR, microRNA; MUT, mutant; Sevo, sevoflurane; WT, wild-type; NS, no significance; ctrl, control.

diseases including Parkinson's and Alzheimer's diseases (36). Thus, the expression level of this protein following cell treatment with sevoflurane was investigated. Western blotting results demonstrated that the treatment with sevoflurane significantly reduced the expression level of OXR1 in HN-h cells.

It is well established that OXR1 is an inducible protein, which is highly expressed in presence of ROS. Its expression enhances ROS scavenging, however due to the necessity of maintaining an equilibrium the protein also has negative regulators that restore an appropriate level of protein expression when the redox equilibrium in the cell is established (35,37). Of these negative-regulators, the 22 nt hsa-miR-302e is involved OXR1 regulation at the post-transcriptional level. The experiments using hsa-miR-302e mimic and inhibitors effectively confirmed that the miR directly targets OXR1 mRNA and downregulates the expression of this gene by annealing to its 3'UTR sequence as demonstrated in the reporter gene expression experiment. Notably, it was demonstrated that sevoflurane treatment increases the expression level of miR-302. As sevoflurane decreased OXR1 expression concomitantly with the induction of miR-302e, it was concluded that sevoflurane induces hsa-miR-302e expression, which in turn downregulates the expression of OXR1. The downregulation of OXR1 disrupts the equilibrium in the cells and the increased the ROS levels leading to the oxidation of cellular proteins and lipids. Oxidative damage results in the activation of different cell death pathways, including apoptosis and necrosis, which are observed as sevoflurane-induced cytotoxicity (38).

High expression of hsa-miR-302e was previously reported to be associated with radio-sensitivity in non-small cell lung cancer (39). To the best of our knowledge the present study is the first to specifically establish experimentally the association of this miR with neuronal cell resistance to oxidative stress. In miR databases, hsa-miR-302e is predicted to target >1,000 human genes, including OXR1. This supports the results of the present study; however, it does not elucidate the mechanism by which sevoflurane influences the expression of this miR. Further investigations will be useful in understanding completely the process by which sevoflurane induces hsa-miR-302e overexpression. The findings of the present study provide a novel opportunity for the treatment and management of diseases associated with oxidative stress in neuronal cells. Deeper investigation of the hsa-miR-302e/OXR1 pathway could give rise to a novel generation of treatments for these diseases.

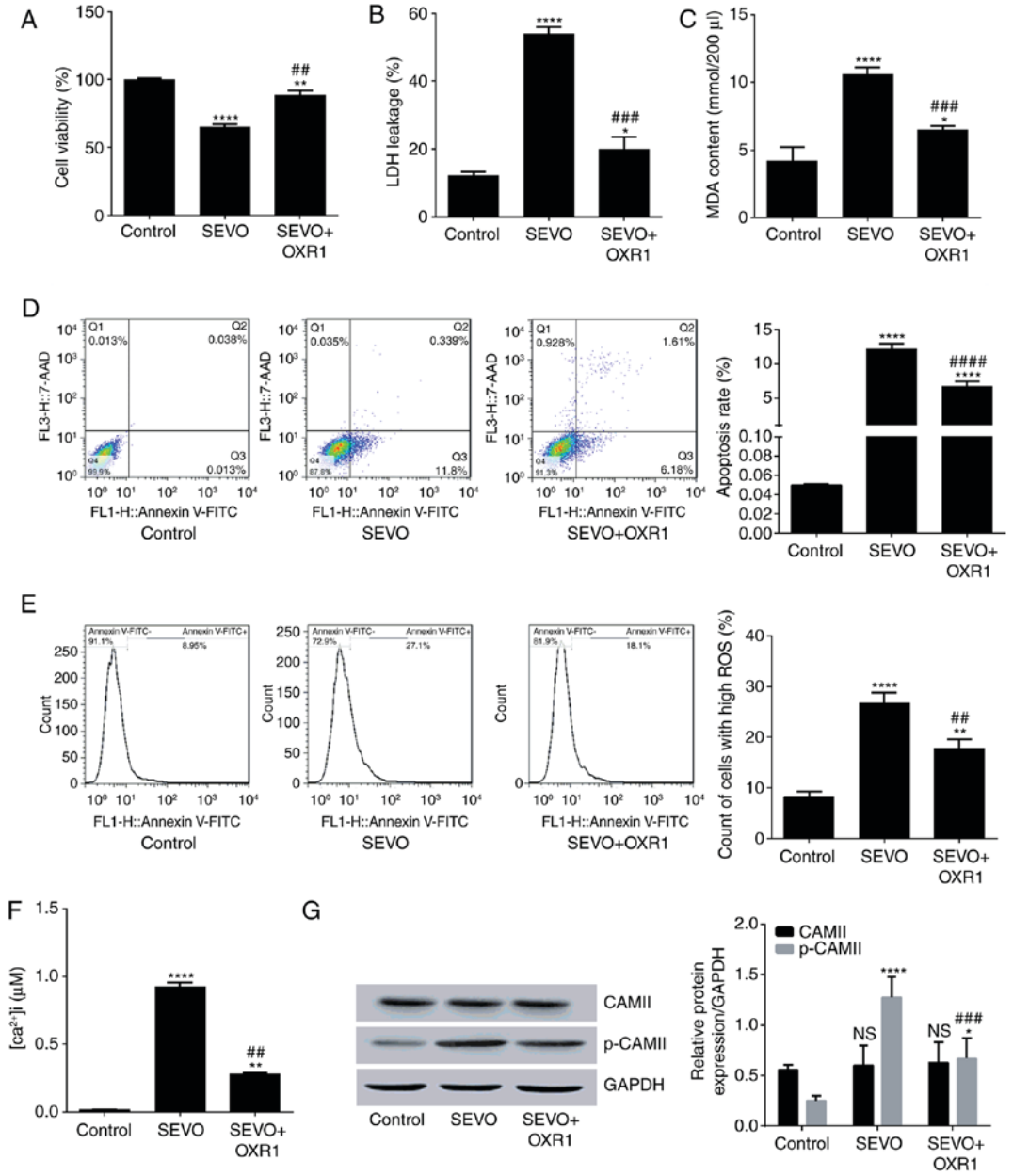

Figure 4. Overexpression of OXR1 abrogates Sevo-induced cytotoxicity. (A) Cell viability determined using an MTT assay. (B) Level of LDH leakage. (C) Results of lipid peroxidation assay (MDA content). (D) Apoptosis rate with flow cytometry results. (E) ROS count. (F) Concentration of intracellular Ca^{2+}. (G) Expression level of CAMII and p-CAMII relative to GAPDH. *P<0.05, **P<0.01, ****P<0.0001 vs. the control; $^{\#\#}$P<0.01, $^{\#\#\#}$P<0.001, $^{\#\#\#\#}$P<0.0001 vs. the Sevo group. Sevo, sevoflurane; OXR1, oxidation resistance gene 1; LDH, lactate dehydrogenase; MDA, malondialdehyde; 7-AAD, 7-aminoactinomycin D; FITC, fluorescein isothiocyanate; ROS, reactive oxidative species; CAMII, calcium/calmodulin-dependent protein kinase II; p-, phospho-; NS, no significance.

Acknowledgements

Not applicable.

Funding

The present study was supported by a grant from the Clinical Scientific Research Project of Wuhan Municipal Health Planning Commission (Wuhan, China; grant no. WX16C06).

Availability of data and materials

The analyzed data sets generated during the study are available from the corresponding author on reasonable request.

Authors' contributions

LY, QS, YX, XL and JP designed the study. LY and QS conducted the experiments and analyzed the data. LY wrote the manuscript. JP supervised the study. All authors read and approved the final manuscript.

Ethics approval and consent to participate

Not applicable.

Patient consent for publication

Not applicable.

Competing interests

The authors declare that they have no competing interests.

References

1. Freiermuth D, Mets B, Bolliger D, Reuthebuch O, Doebele T, Scholz M, Gregor M, Haschke M, Seeberger MD and Fassl J: Sevoflurane and isoflurane-pharmacokinetics, hemodynamic stability, and cardioprotective effects during cardiopulmonary bypass. J Cardiothorac Vasc Anesth 30: 1494-1501, 2016.
2. Likhvantsev VV, Landoni G, Levikov DI, Grebenchikov OA, Skripkin YV and Cherpakov RA: Sevoflurane vs. total intravenous anesthesia for isolated coronary artery bypass surgery with cardiopulmonary bypass: A randomized trial. J Cardiothorac Vasc Anesth 30: 1221-1227, 2016.
3. Ružman T, Šimurina T, Gulam D, Ružman N and Miškulin M: Sevoflurane preserves regional cerebral oxygen saturation better than propofol: Randomized controlled trial. J Clin Anesth 36: 110-117, 2017.
4. Walia H, Ruda J and Tobias JD: Sevoflurane and bradycardia in infants with trisomy 21: A case report and review of the literature. Int J Pediatr Otorhinolaryngol 80: 5-7, 2016.
5. Conreux F, Best O, Preckel MP, Lhopitault C, Beydon L, Pouplard F and Granry JC: Effets électroencéphalographiques du sévoflurane à l'induction chez le jeune enfant: Étude prospective sur 20 cas. Ann Fr Anesth Réanim 20: 438-445, 2001 (In French).
6. Geng YJ, Wu QH and Zhang RQ: Effect of propofol, sevoflurane, and isoflurane on postoperative cognitive dysfunction following laparoscopic cholecystectomy in elderly patients: A randomized controlled trial. J Clin Anesth 38: 165-171, 2017.
7. Xiao H, Liu B, Chen Y and Zhang J: Learning, memory and synaptic plasticity in hippocampus in rats exposed to sevoflurane. Int J Dev Neurosci 48: 38-49, 2016.
8. Hu N, Wang M, Xie K, Wang H, Wang C, Wang C, Wang C, Li Y, Yu Y and Wang G: Internalization of GluA2 and the underlying mechanisms of cognitive decline in aged rats following surgery and prolonged exposure to sevoflurane. Neurotoxicol 49: 94-103, 2015.
9. Shen X, Liu Y, Xu S, Zhao Q, Guo X, Shen R and Wang F: Early life exposure to sevoflurane impairs adulthood spatial memory in the rat. Neurotoxicol 39: 45-56, 2013.
10. Wu Y, Gu C and Huang X: Sevoflurane protects against hepatic ischemia/reperfusion injury by modulating microRNA-200c regulation in mice. Biomed Pharmacother 84: 1126-1136, 2016.
11. Sun Y, Li Y, Liu L, Wang Y, Xia Y, Zhang L and Ji X: Identification of miRNAs involved in the protective effect of sevoflurane preconditioning against hypoxic injury in PC12 cells. Cell Mol Neurobiol 35: 1117-1125, 2015.
12. Yi W, Li D, Guo Y, Zhang Y, Huang B and Li X: Sevoflurane inhibits the migration and invasion of glioma cells by upregulating microRNA-637. Int J Mol Med 38: 1857-1863, 2016.
13. Ye J, Zhang Z, Wang Y, Chen C, Xu X, Yu H and Peng M: Altered hippocampal microRNA expression profiles in neonatal rats caused by sevoflurane anesthesia: MicroRNA profiling and bioinformatics target analysis. Exp Ther Med 12: 1299-1310, 2016.
14. Fujimoto S, Ishikawa M, Nagano M and Sakamoto A: Influence of neonatal sevoflurane exposure on nerve development-related microRNAs and behavior of rats. Biomed Res 36: 347-355, 2015.
15. Friedman R, Farh K, Burge C and Bartel D: Most mammalian mRNAs are conserved targets of microRNAs. Genome Res 19: 92-105, 2009.
16. Winter J, Jung S, Keller S, Gregory R and Diederichs S: Many roads to maturity: MicroRNA biogenesis pathways and their regulation. Nat Cell Biol 11: 228-234, 2009.
17. Wang Q, Li G, Li B, Chen Q, Lv D, Liu J, Ma J, Sun N, Yang L, Fei X and Song Q: Sevoflurane represses the self-renewal ability by regulating miR-7a,7b/Klf4 signalling pathway in mouse embryonic stem cells. Cell Prolif 49: 609-617, 2016.
18. Zhou C, Gu H, Fan R, Wang B and Lou J: MicroRNA 302/367 cluster effectively facilitates direct reprogramming from human fibroblasts into functional neurons. Stem Cells Dev 24: 2746-2755, 2015.
19. Zhang Z, Hong Y, Xiang D, Zhu P, Wu E, Li W, Mosenson J and Wu WS: MicroRNA-302/367 cluster governs hESC self-renewal by dually regulating cell cycle and apoptosis pathways. Stem Cell Reports 4: 645-657, 2015.
20. Li HL, Wei JF, Fan LY, Wang SH, Zhu L, Li TP, Lin G, Sun Y, Sun ZJ, Ding J, *et al*: miR-302 regulates pluripotency, teratoma formation and differentiation in stem cells via an AKT1/OCT4-dependent manner. Cell Death Dis 7: e2078, 2016.
21. Gao Z, Zhu X and Dou Y: The miR-302/367 cluster: A comprehensive update on its evolution and functions. Open Biol 5: 150138, 2015.
22. Yang CM, Chiba T, Brill B, Delis N, von Manstein V, Vafaizadeh V, Oellerich T and Groner B: Expression of the miR-302/367 cluster in glioblastoma cells suppresses tumorigenic gene expression patterns and abolishes transformation related phenotypes. Int J Cancer 137: 2296-2309, 2015.
23. Maadi H, Moshtaghian A, Taha MF, Mowla SJ, Kazeroonian A, Haass NK and Javeri A: Multimodal tumor suppression by miR-302 cluster in melanoma and colon cancer. Int J Biochem Cell Biol 81: 121-132, 2016.
24. Parchem RJ, Moore N, Fish JL, Parchem JG, Braga TT, Shenoy A, Oldham MC, Rubenstein JL, Schneider RA and Blelloch R: miR-302 is required for timing of neural differentiation, neural tube closure, and embryonic viability. Cell Rep 12: 760-773, 2015.
25. Suresh B, Kumar AM, Jeong HS, Cho YH, Ramakrishna S and Kim KS: Regulation of Fanconi anemia protein FANCD2 monoubiquitination by miR-302. Biochem Biophys Res Commun 466: 180-185, 2015.
26. Yang SL, Yang M, Herrlinger S, Liang C, Lai F and Chen JF: MiR-302/367 regulate neural progenitor proliferation, differentiation timing, and survival in neurulation. Dev Biol 408: 140-150, 2015.
27. Li HH, Lin SL, Huang CN, Lu FJ, Chiu PY, Huang WN, Lai TJ and Lin CL: miR-302 attenuates amyloid-beta-induced neurotoxicity through activation of Akt signaling. J Alzheimers Dis 50: 1083-1098, 2016.
28. Fang YC and Yeh CH: Inhibition of miR-302 suppresses hypoxia-reoxygenation-induced H9c2 cardiomyocyte death by regulating Mcl-1 expression. Oxid Med Cell Longev 2017: 7968905, 2017.
29. Ghasemi-Kasman M, Baharvand H and Javan M: Enhanced neurogenesis in degenerated hippocampi following pretreatment with miR-302/367 expressing lentiviral vector in mice. Biomed Pharmacother 96: 1222-1229, 2017.
30. Ghasemi-Kasman M, Shojaei A, Gol M, Moghadamnia AA, Baharvand H and Javan M: miR-302/367-induced neurons reduce behavioral impairment in an experimental model of Alzheimer's disease. Mol Cell Neurosci 86: 50-57, 2018.
31. Zhou YF, Wang QX, Zhou HY and Chen G: Autophagy activation prevents sevoflurane-induced neurotoxicity in H4 human neuroglioma cells. Acta Pharmacol Sin 37: 580-588, 2016.
32. Livak KJ and Schmittgen TD: Analysis of relative gene expression data using real-time quantitative PCR and the 2(-Delta Delta C(T)) method. Methods 25: 402-408, 2001.
33. Altuntas TG, Zager RA and Kharasch ED: Cytotoxicity of S-conjugates of the sevoflurane degradation product fluoromethyl-2,2-difluoro-1-(trifluoromethyl) vinyl ether (Compound A) in a human proximal tubular cell line. Toxicol Appl Pharmacol 193: 55-65, 2003.
34. Manoharan S, Guillemin GJ, Abiramasundari RS, Essa MM, Akbar M and Akbar MD: The role of reactive oxygen species in the pathogenesis of Alzheimer's disease, Parkinson's disease, and Huntington's disease: A mini review. Oxid Med Cell Longev 2016: 8590578, 2016.
35. Liu KX, Edwards B, Lee S, Finelli MJ, Davies B, Davies KE and Oliver PL: Neuron-specific antioxidant OXR1 extends survival of a mouse model of amyotrophic lateral sclerosis. Brain 138: 1167-1181, 2015.
36. Oliver PL, Finelli MJ, Edwards B, Bitoun E, Butts DL, Becker EB, Cheeseman MT, Davies B and Davies KE: Oxr1 is essential for protection against oxidative stress-induced neurodegeneration. PLoS Genet 7: e1002338, 2011.
37. Finelli MJ, Sanchez-Pulido L, Liu KX, Davies KE and Oliver PL: The evolutionarily conserved Tre2/Bub2/Cdc16 (TBC), lysin motif (LysM), domain catalytic (TLDc) domain is neuroprotective against oxidative stress. J Biol Chem 291: 2751-2763, 2016.
38. Wu Y, Davies KE and Oliver PL: The antioxidant protein Oxr1 influences aspects of mitochondrial morphology. Free Radic Biol Med 95: 255-267, 2016.
39. Chen X, Xu Y, Liao X, Liao R, Zhang L, Niu K, Li T, Li D, Chen Z, Duan Y and Sun J: Plasma miRNAs in predicting radiosensitivity in non-small cell lung cancer. Tumour Biol 37: 11927-11936, 2016.